CHAPTER 1

1.1 Introduction

The ultraviolet (UV) region of electromagnetic radiation occupies a section of wavelengths ranging from 400 to 10 nm [1]. It is highly ionizing and activates many chemical processes on different types of materials and living beings. It is divided into four categories: near UV with wavelength range 400 to 300 nm, middle UV from 300 to 200 nm, far or vacuum UV from 200 to 100 nm and extreme UV from 100 to 10 nm. The lower wavelength radiation that generally reaches the earth's surface is the first mentioned. Middle UV radiation is absorbed by the ozone layer while far UV radiation is absorbed by molecular oxygen. Extreme UV radiation is absorbed by all types of atomic and molecular gases and is not supposed to reach the earth's surface at all. As a function of its effects on the biosphere, the UV regions are arbitrarily called: UVA from 400–320 nm, UVB from 320-280 nm and UVC from 280-180 nm [2]. The different regions for the UV section of the electromagnetic spectrum are shown in Table 1.1 below.

Table 1.1: UV radiation wavelength range and corresponding names [2].

Category	Wavelength (nm)	Category	Wavelength (nm)
UV - A	400 – 320/315	**Near UV**	400 – 300
UV - B	315/320 – 280	**Middle UV**	300 – 200
UV - C	280 – 180	**Far UV**	200 – 122/100
Vacuum UV	200 – 10	**Extreme UV**	121/100 – 10

Further classification of the radiation wavelength is termed the solar-blind and visible blind regions. Some UV radiation from the sun is absorbed by the ozone in a certain range of wavelengths, thus not reaching the earth's atmosphere. Figure 1.1 indicates this condition with a comparison between the regions above and below the atmosphere. Some detectors require that the UV signal be detected in the background of the sun. It is evident from the figure that the amount of solar radiation reaching the earth's surface drops greatly around 300 nm (4.1 eV). Thus a solar blind detector detects UV radiation below 300 nm. The wavelength range of AlGaN makes it possible to have both visible-blind and solar blind UV detectors, depending on the energy of the radiation to be detected.

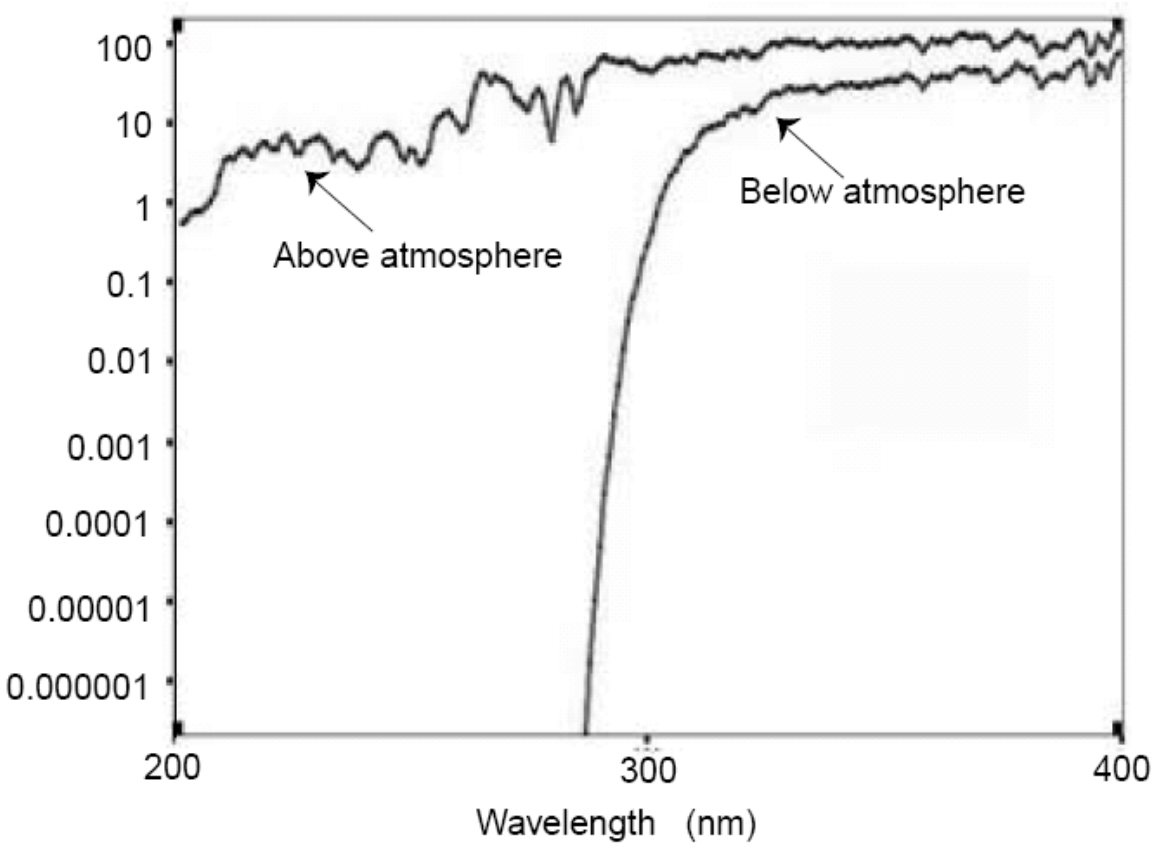

Figure 1.1: Solar UV above and below the atmosphere of the earth, from 1976 US standard atmosphere [3].

In addition, figure 1.2 clearly depicts the solar blind and visible blind regions. Visible blind indicates those regions where UVB radiation is active while solar blind refers to the regions where UVC is dominant. UVB never reach the earth surface in general, but due to ozone layer depletion, there may be some effects of on the biosphere.

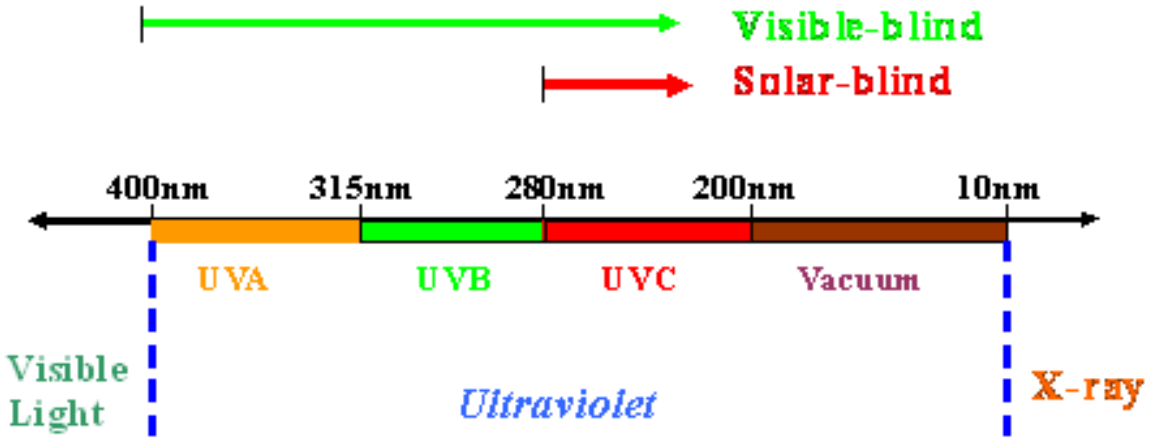

Figure 1.2: Regions of electromagnetic radiation, showing the different ultraviolet sections and their borders [4].

The main source of UV radiation is the sun. The energy per unit of time reaching the earth at right angles to the light rays that are observed outside the earth's atmosphere is 1353 W/m^2, of which only 121.8 W/m^2 (9%) constitute the total UV radiation [4]. The UV radiation on earth and its effects depend on the solar altitude angle lying between any line directed to the sun and the projection on the horizontal plane. Thus the amount of UV radiation at different places on the earth depends on the position of the sun during the day and the season of year. Research in Germany has shown that a decline in the amount of ozone has been observed to be high in spring, indicating an increase in UV radiation at that time of the year [5]. UV radiation is also produced artificially from electroluminiscence of certain types of matter, when ions, atoms and molecules are accelerated at high voltages.

A global scale called Solar Ultra Violet Index (UVI) is used to describe the level of UV radiation on the biosphere; it is usually seen on TV during the weather forecast. The UVI is a form of

warning to mankind to protect oneself against such a radiation effect. The values range from zero to ten and above, indicating the strength of UV radiation. These values depend on the geographical region and time of day [6]. In many places, the UVI is very high around midday and it is required that one must be protected from the effects of the sun. When the UVI is less than three, a person may be free from these harmful effects, but anything above this calls for protection.

The effects of UV radiation on the biosphere lead to issues such as sunburn, skin cancer and eye cataracts. Sunscreens, hats and sunglasses are used together for maximum protection from UV radiation. Issues with regards to these protection systems include the correct amount of sunscreen protection, known as the Sun Protection Factor (SPF), in the solutions that are applied. The values differ from skin to skin and from person to person. A common practice amongst some fair skinned people is to expose themselves to UV radiation in order to pigment their skin. Overexposure may lead to erythema and premature aging, which may be followed by skin cancer and eye cataracts [7]. Snow, white sand, water and any similar substances increase one's UV exposure by reflection and this is not good for one's eyes.

However, UV radiation effects are beneficial to humankind well being in terms of the activation of vitamin D, the most important of sun energy and stimulation of photosynthesis [8]. Sterilization of water and the removal of micro-organisms from foods and in the pasteurization process require the use of UV radiation. Such radiation is used in modern refrigeration to keep food and air free of micro-organisms during long storage, giving them longer life. In biotechnology, UV radiation is used in the synthesis of vitamins D_2 and D_3. In addition, UV flytraps are used to control pests, killing them through shock once attracted to the light.

UV detection has been achieved by photomultiplier tubes (PMT), thermal detectors, and charged-coupled devices (CCD). PMT displays high gain and low noise and can reduce the infiltration of low energy photons, but these are large fragile instruments that require much power. Thermal detectors such as pyrometers and bolometers are used in the calibration processes of UV detectors, but are slow and their response is wavelength independent. Semiconductor photodiodes and CCDs are narrow bandgap solid-state devices that require

moderate bias. As solid-state devices, photodetectors are small, lightweight and insensitive to magnetic fields. Their low-cost, good linearity and sensibility, and capability of high-speed operation make them suitable for UV detection. Si, GaAs, and GaP have been used in the fabrication of UV detectors [9]. These materials are suitable for devices operating in the visible and infrared sections of the electromagnetic radiation. UV detectors made from these materials need filters to stop interference of low energy radiation.

The most common semiconductor UV enhanced devices are made of Si, displaying some limitations due to the narrow and indirect bandgap of Si. Si-based UV photodiodes have been made as p-n junction photodiodes and charge inversion photodiodes. In p-n-junction UV photodiodes, the junction is typically situated at a depth of 0.2 µm and the devices are coated with a SiO_2 surface layer, acting as surface passivation and anti-reflection coating [10]. The charge inversion photodiodes are similar to metal-oxide semiconductor structures designed for field effect transistors. Photodetection occurs as a result of the presence of the electric field at the Si/SiO_2 interface. This is the region of high UV radiation absorption and requires control of the surface recombination at the Si/SiO_2 interface, which is very critical for the performance of the device. Si, GaP, CsI and GaAs-based UV detectors suffer radiation aging, as their bandgap is far lower than the UV photon energies.

Diamond, SiC, GaN and ZnO are wide bandgap (WBG) semiconductors suitable for the fabrication of UV detectors [11]. The wide bandgap is itself an important advantage for UV detectors because it enables room-temperature operation and provides important intrinsic visible blindness. Thermal conductivity of the wide bandgap materials is very high compared to that of Si, which renders devices suitable to operate in high temperature and high power environments. Electron velocities of the WBG semiconductors are lower than those of conventional semiconductors, but at high electric fields, these become larger. A further interesting feature of WBG semiconductors for operation in the lower wavelengths of the electromagnetic spectrum is the ability to display negative electron affinity [12], which makes electrons readily available when the semiconductor interacts with appropriate photon energies. In this thesis, GaN-based materials are used in the study of ultraviolet detectors.

1.2 Aims of the study

In this work, the focus falls on the optimization of Schottky diodes suitable for use as UV detectors on GaN-based semiconductors. The performance of metal contacts on semiconductors depends on the quality of the surface prior to metallization, the chemicals used in preparing the surface, the morphology of the surface, the adhesion of the metal to the semiconductor, reproducibility, resistance to radiation damage and thermal stability. The aims of the study were to establish the following:

- Cleaning procedures for GaN for the purpose of metallization.
- GaN for device patterning using wet etch processes.
- Choosing a metal contact with high UV light transmission.
- Fabrication of Schottky barrier UV detectors.
- Setting-up an electro-optical characterization station for the evaluation of the UV detectors.

1.3 Synopsis of the thesis

The focus of this work has been described. This chapter serves as a prelude to the GaN UV detectors and offers the motivation for the study. Chapter 2 consists of the literature review on GaN semiconductors for UV detectors. Chapter 3 presents a theoretical overview of Schottky Barrier diodes, while Chapter 4 contains the experimental details of the research. Chapter 5 furnishes the results of all experiments and Chapter 6 presents the conclusions.

REFERENCES

[1] Razeghi M. and Rogalski A., Journal of Applied Physics **79** (1996) 7433.

[2] Goldberg Y. A., Semiconductor Science and Technology, **14** (1999), R41.

[3] Parish G., PhD Thesis, University of Santa Barbara (2001)

[4] Coulson K. L, Solar and Terrestrial Radiation, Academic Press, New York (1975).

[5] Winkler P. and Trepte S., Gesundhetswesen, Suppl. **66** (2004) S31.

[6] Koepke P., De Backer H., Ericson P., Feister U., Grifoni D., Koskela T., Lehman A., Lityska Z., Oppenrieder A., Staiger H. and Vanicek K., UV Index Photobiology, International Radiation Symposium (2000).

[7] Mackie R. M., Progress in Biophysics and Molecular Biology, **92** (2006) 92.

[8] Schmalwieser A. W. and Schauberger G., ICB2005, Garmisch-Partenkirchen, Germany

[9] Rogalski A., Progress in Quantum Electronics **27** (2003) 59.

[10] Korde R. and Geist J., Applied Optics **26** (1987) 5284.

[11] Monroy E., Omness F. and Calle F., Semiconductor Science and Technology **18** (2003) R33.

[12] Nemanich R. J., English S. L., Hartman J. D., Sowers A. T., Ward B. L., Ade H. and Davies R. F., Applied Surface Science **146** (1999) 287.

CHAPTER 2

GaN-based materials for Ultraviolet Detectors

2.1 Introduction

In this chapter, the basic information about GaN-based materials is presented. The issues that affected the development of GaN are discussed in section 2.2. This is followed by a discussion of the properties and applications of GaN-based materials. Finally, a review of AlGaN photodiodes is done.

2.2 Progressive development of GaN-based materials

GaN is one of the most successful materials used to make optoelectronic devices operating in the blue and ultraviolet region (UV) of the electromagnetic spectrum. Most colours in the visible range have been covered by other semiconductors with Si and GaP containing devices operating in the infrared (IR) region. Since the 1990s, there has been notable growth in the research and development of GaN devices [1]. However, the success of such devices has been limited by material issues such as the presence of high-unintended donor concentrations [2], lack of suitable substrates [3] and growth methods. These issues resulted in dislocation densities as high as 1×10^{10} cm^{-2}, leading to uncontrollable electronic properties in GaN crystals [4,5]. Similarly, AlN and InN suffered in the same manner in their development, and both are useful in bandgap engineering, producing AlGaN and InGaN respectively. In and Al content in GaN can be tailored to select a specific wavelength for device fabrication [6]. InGaN and AlGaN are used to introduce green and UV wavelengths respectively. Figure 2.1 presents a graph of bandgap tuning with Al and In in GaN. SiC, diamond, and ZnO are inserted for comparison.

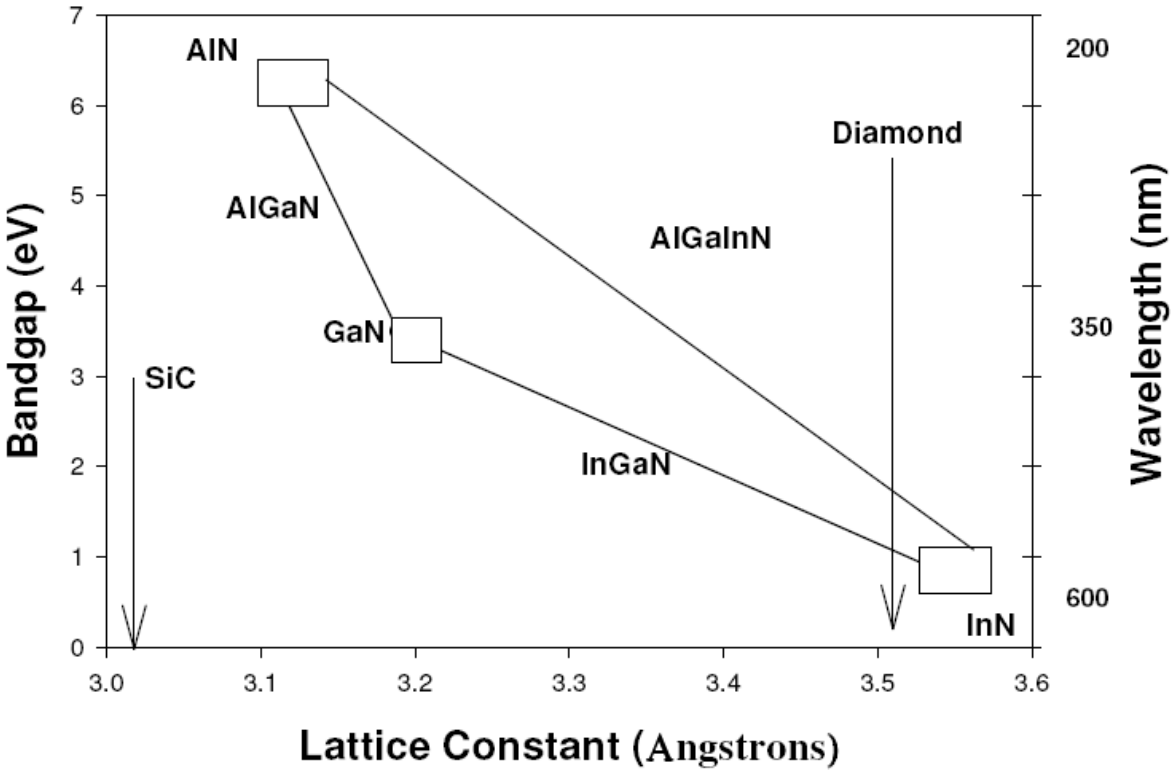

Figure 2.1: Bandgap of GaN-based materials for UV detectors. SiC, ZnO and diamond are inserted for comparison.

2.2.1 Growth methods

In an effort to improve the quality of GaN crystals and reduce dislocation density, several growth methods were used. The growth methods that have been used are vapour phase epitaxy (VPE), which includes both hydride (HVPE) [7] and metal organic vapour phase epitaxy (MOVPE) [8], and molecular beam epitaxy (MBE) [9]. MOVPE is a chemical vapour deposition method, also termed metal organic chemical vapour deposition (MOCVD), organometallic chemical vapour deposition (OMCVD) or organometallic vapour phase epitaxy (OMVPE). This method uses ammonia (NH_3) and trimethyllgallium (TMG) as precursors for nitrogen and gallium, respectively. In the case of other nitrides, trimethyllaluminium (TMAl) and trimethylinduim (TMIn) are used as sources for Al in AlN and In in InN, respectively. The chemical equation for the growth of GaN is given by:

$$Ga(CH_3)_3 + NH_3 \rightarrow GaN + CH_4 \quad (2.1)$$

The MOCVD method requires a high partial pressure for NH_3 and a high growth temperature, ranging from 1000 to 1100°C. The first step is growing the material at low temperature producing GaN crystallites that covers the substrate. The final film is grown at a higher temperature to control and reduce contamination in the material. GaN is doped with Si or Mg for n-type and p-type doping. In n-type doping, Si is sourced from methyl silane, while in p-type doping Mg is sourced from biscyclopentadithyl. Figure 2.2 shows the growth process of the III-Nitrides. The carrier gas introduces the required element for the growth of GaN and the by products are expelled from the system, with the semiconductor growing onto a substrate.

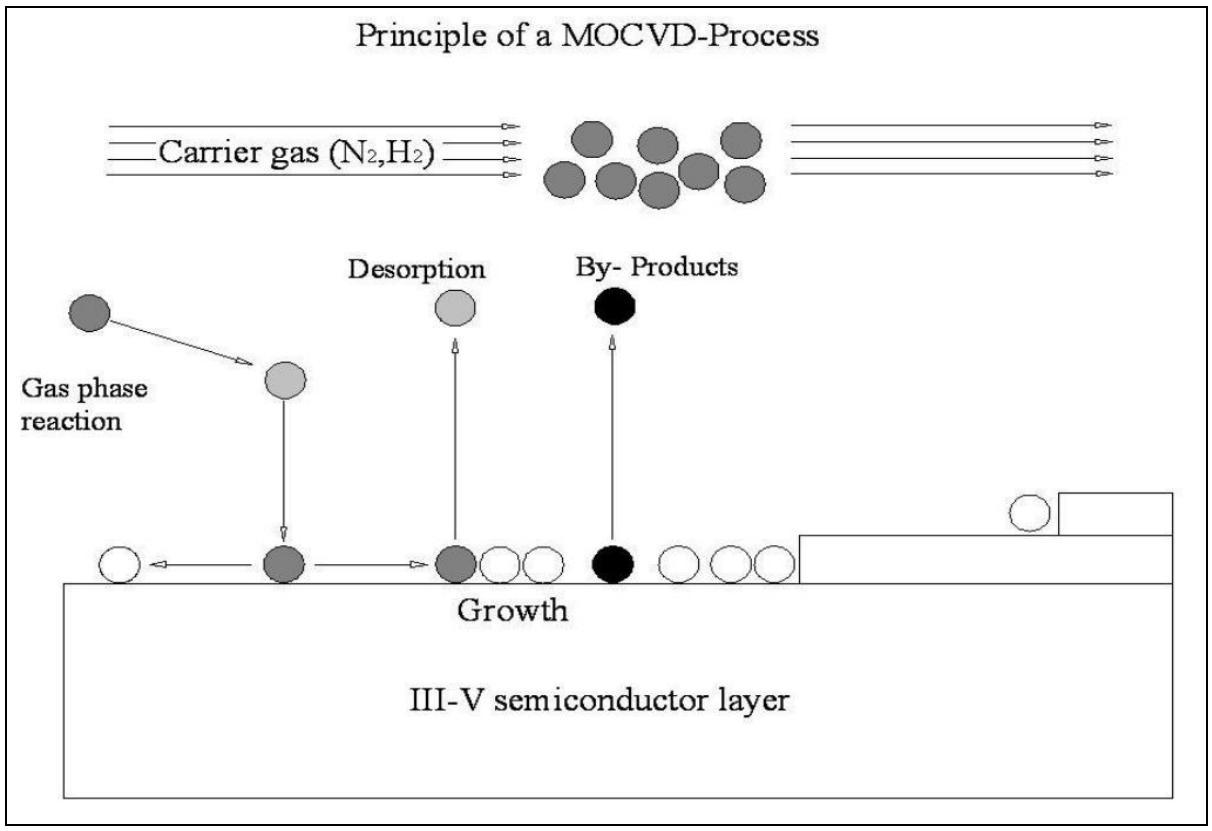

Figure 2.2: MOCVD growth process for III-Nitrides.

MBE is an ultra high vacuum technique for growing semiconductor crystals. High purity Ga is heated in an effusion cell until it evaporates and deposits slowly onto a substrate. Nitrogen atoms are supplied from a plasma source. The growth of GaN is controlled by conditions that allow

atoms of Ga and N to be deposited layer by layer onto a heated substrate. The MBE method operates in an ultra high vacuum chamber to minimize crystal contamination during growth. This method is capable of producing heterostructures with sharp interfaces and of growing zinc-blende structure GaN (normally, GaN is grown in a wurtzite structure). The chamber is also equipped with Si, Mg, In and Al effusion cells for alloying purposes. The disadvantage of the MBE method is the low growth temperature, 700 to 800°C as compared to MOCVD where temperatures are 1000 to 1100°C. GaN is a thermodynamically unstable material in a vacuum and the thin film may decompose into Ga and N in the MBE, when the deposition rate becomes lower than the decomposition rate due to a temperature difference between the chamber and the substrate. The low substrate temperature reduces surface atom mobility, resulting in increased densities of defects [10]. Figure 2.3 shows the schematics of the MBE growth method.

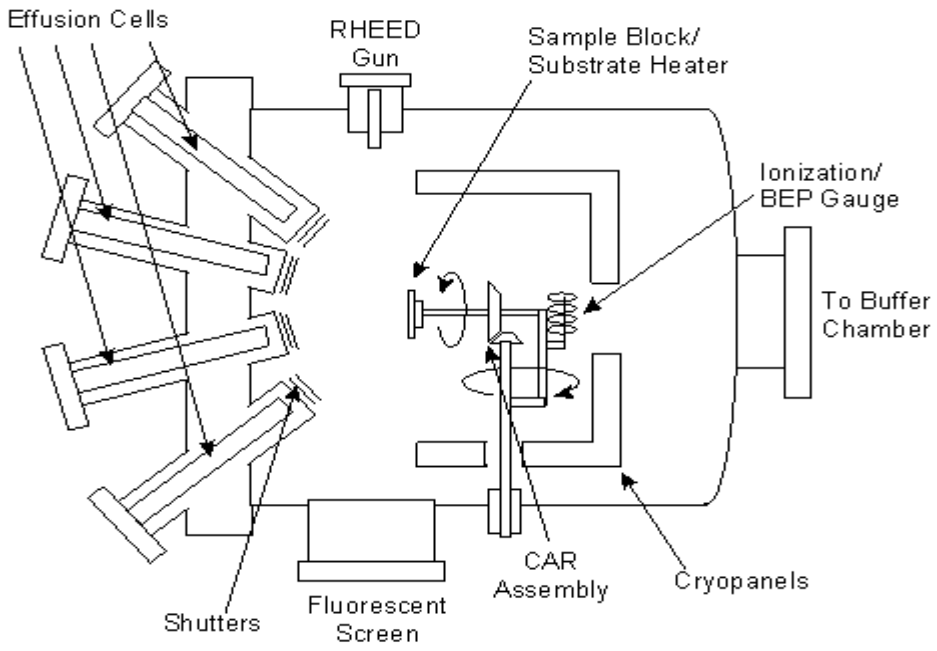

Figure 2.3: MBE growth process for III-Nitrides [11].

2.2.2 Substrates for GaN

In addition to the growth method, the crystal quality of semiconductors depends on the suitability of the substrate. In growing GaN, sapphire (α-Al_2O_3), GaAs, Si, SiC, $LiGaO_2$, $LiAlO_2$ and ZnO have been used as a substrate [3]. The criterion for choosing a suitable substrate is lattices match. In addition, practical properties such as crystal structure, surface finish and composition, chemical, thermal and electrical properties are also considered. Currently, it has become important to study the effects of treatments of a substrate (e.g. heating or chemical processing) prior to the deposition of GaN. For example, it has been shown that wet etching of sapphire prior to the deposition of GaN crystals reduces threading dislocations [12]. α-Al_2O_3 has been extensively used as a substrate for GaN. It has a crystal orientation parallel to GaN c-plane, and the lattice mismatch is about 15 %, leading to a dislocation density of about 10^{10} cm^{-2}. α-Al_2O_3 has a rhombohedral structure and is highly anisotropic. Like GaN, it exhibits extremely high chemical and thermal stability with a melting point of 2040 °C. Its bandgap of 9.1 eV permits excellent optical transmission. Furthermore, the coefficient of the thermal expansion of α-Al_2O_3 is greater than that of GaN, resulting in comprehensive stress in the grown film during cooling. Such stress causes cracks in both GaN and α-Al_2O_3.

A continually improving technique to produce GaN with less threading dislocations is the epitaxial lateral overgrowth (ELOG), considered to be an alternative substrate [13]. Figure 2.4 depicts the schematics of the ELOG substrate. The ELOG technique takes advantage of the large anisotropy of the GaN growth rate in the [0001] direction, controlling dislocations through the patterned substrate such that they do not reach the surface of the final layer as shown in figure 2.4 (D). GaN thin buffer layer is grown on sapphire as a usual practice for GaN growth as shown in figure 2.4 (A). A dielectric material such as SiO_2 or SiN mask is then patterned onto the GaN buffer layer {figure 2.4 (B)}. The thin film is then grown onto the patterned GaN buffer layer {figure 2.4 (C)}. Using MOCVD, ELOG and several of its variations has been shown to significantly reduce the dislocation density of GaN crystals to as low as 10^6 cm^{-3} [14].

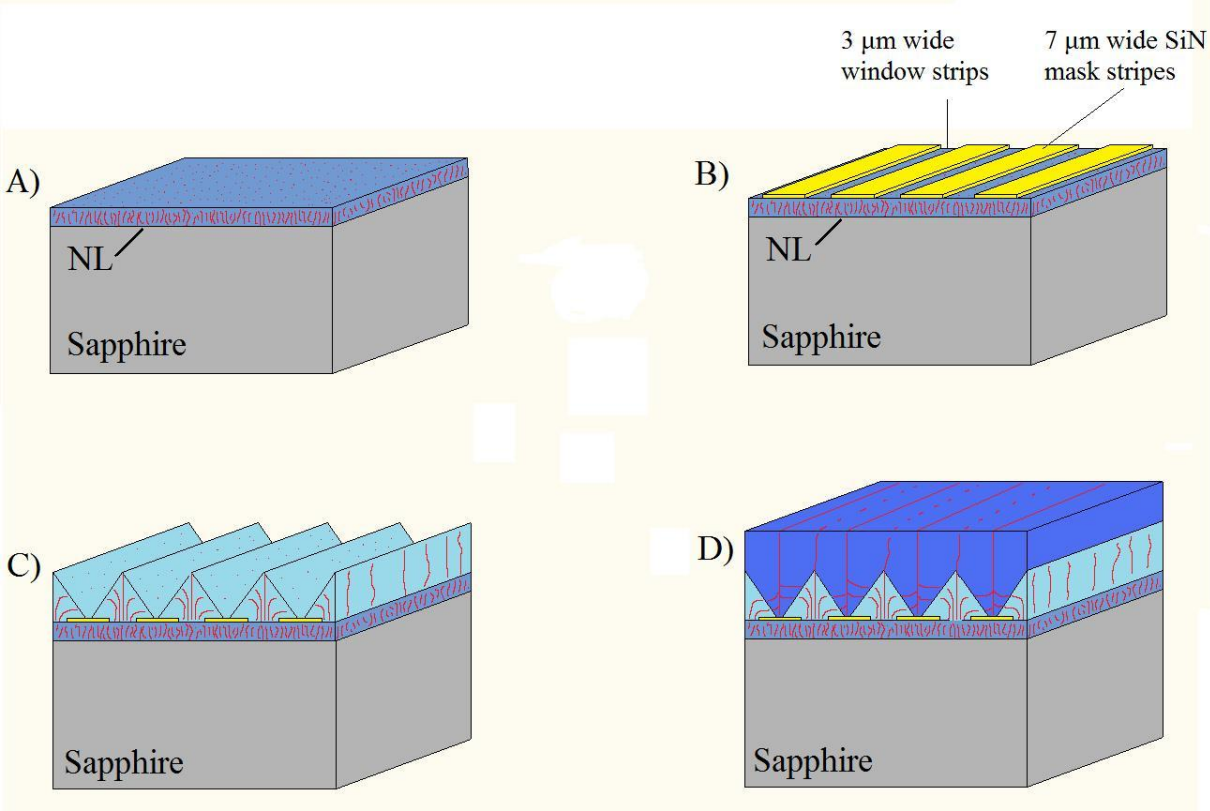

Figure 2.4: Schematic representations of 2 step ELOG for GaN, where NL is the GaN nucleation layer [13].

2.2.3 High n-type Conductivity

The first GaN crystals were observed to possess high n-type conductivity, which was attributed to nitrogen vacancies. This is an unresolved issue in GaN research. Published reports [15,16,17,18] suggest impurities such as Si, C, O, and H as being responsible for n-type conductivity. Park et al. have reported that Si and C are responsible for n-type doping in GaN films [15], where C atoms are acting as compensating acceptors in the crystal, influencing the electron concentration. Van de Walle et al. reported that O, a shallow donor in GaN, is responsible for high background n-type conductivity while Zhang et al. claim that H is responsible for this phenomenon [16,17]. In addition to n-type conductivity, there is a strong presence of parasitic yellow band (YB) luminescence associated with point defects in GaN crystals. Ogino et al. suggested that the YB is a transition that takes place between a shallow donor and a deep accepter level [18]. This suggestion was demonstrated by Saarinen et al. using

positron annihilation spectroscopy, and they concluded that the intensity of YB is directly proportional to the concentration of Ga vacancies [19]. Reynolds et al. have studied the source of yellow luminescence in GaN. They concluded that Ga vacancies, in partnership with the O atom at a nitrogen site, are responsible for point defects producing the YB [20]. More recently, researchers have again suggested that the YB is associated with O impurities in GaN [21]. Related to the impurities discussed above, defects have been studied using Deep Level Transient Spectroscopy (DLTS), which identified vacancies and interstitials in semiconductors. Defects in materials act as electron and hole traps, affecting the current transport in devices. In HVPE grown GaN, three electron traps have been shown by DLTS: E1, E2 and E3 with activation energies 0.264, 0.580 and 0.665 eV [22], with E1 and E2 appearing in concentrations above 2 X $10^{13}cm^{-3}$ in MOVPE [23]. Auret et. al. have also reported two electron traps, E_c - 0.23 eV and E_c - 0.58 eV, in non-intentionally doped MOVPE GaN with activation energies 0.27 and 0.61 eV [24].

2.2.4 Doping of GaN

Doping of GaN plays a crucial role in the performance of devices as it alters GaN's electrical properties by enhancing its conductivity. Using Si in n-type doping of GaN, a carrier density as high as 2.2 x 10^{19} cm^{-3} and a Hall mobility of 287 cm^2/Vs have been recorded [25]. In addition, Si doping has led to a reduction of threading dislocation density in GaN, through the formation of SiN, which stops the propagation of edge dislocation from reaching the surface of the crystal.]. In the case of p-type doping, group II elements like Mg, Be, Ca, Zn, and a combination of Mg and Be have been used. Mg doping is the most efficient, allowing the production of semi-insulating p-type crystals. The highest carrier density in Mg doped GaN has been recorded as 8 x 10^{18} cm^{-3} with the correspondingly low resistivity of 0.8 Ω cm. For p-GaN growth with Ga-polarity, the incorporation of Mg has a tendency to introduce stacking faults, thus inverting the polarity to N-face, and reducing threading dislocation from reaching the surface [26]. These are also defects introduced into the material which exert adverse effects on the performance of devices.

2.2.5 Effects of defects in GaN devices

GaN, like all semiconductors, contains defects due to growth conditions, method of growth, doping, and the substrate used. Dislocations are observed directly from the substrate where the growth begins from a low temperature nucleation layer. Growth processes with both the continuous nucleation layer and the one formed by isolated islands end with vertical threading dislocations. Dislocations in GaN are identified as edge-type, screw type and mixed character type. All these defects influence device performance, including the different types of photodiodes. GaN photodiodes are characterized by high gain, long response time and a responsivity that is dependent on frequency and optical power. Gain is defined as the ratio of the excess–carrier recombination lifetime and the electron transit time across the diode. Since electrons have very high mobility in GaN, high gain will be affected by a long stay of carriers in traps, reducing the probability of recombination. High gain thus occurs at the expense of the long response time of minority carriers. Published works have attributed the mechanism of the long response times and high gain in n-type GaN photoconductors to acceptor levels trapping the photogenerated holes [27, 28, 29]. Traps in the semiconductor material occur as a result of both point defects and dislocations. Hole traps can be reduced by altering the growth conditions for GaN-based materials, and this has proved to have an effect on the photoresponse [30]. Leakage currents in photodiodes consist of the dark current at the reverse bias and have different sources. Surface leakage currents result from surface states and tunneling induced near the surface, and is reduced by surface chemical treatments including passivation. Passivation is responsible for tying up dangling bonds and thus reduces the density of surface states. Reduced leakage currents have been reported in devices grown on ELOG GaN p-n structures and Schottky photodiodes, which are characterized by reduced threading dislocation densities [31]. Low leakage current improves the response time and sharpness of the cut-off wavelength in ELOG GaN [32].

2.3 Properties of GaN-based materials

GaN, with its famous nitride family, AlN and InN, are wide band gap semiconductors that occur in both zincblende and wurtzite structures. Figure 2.5 shows the schematics of GaN wurtzite structure, showing the Ga-face and the n-face. In wurtzite form, the direct band gap of GaN is recorded at 3.5 eV while that of AlN is 6.23 eV [33]. The bandgap of InN was recorded earlier as 1.9 to 2.05 eV [34] while more recently, a new band gap of 0.7 to 1.0 eV [35] was recorded. In cubic form the bandgaps of GaN and AlN are direct while that of InN is indirect [36]. Alloying GaN with InN and AlN allows for the tuning of band gaps and emission wavelengths. AlGaN is suitable for the fabrication of UV solar-blind detectors. By varying the Al content, the responsivity cut-off wavelength can be varied from 280 nm [37] to as low as 240 nm [38].

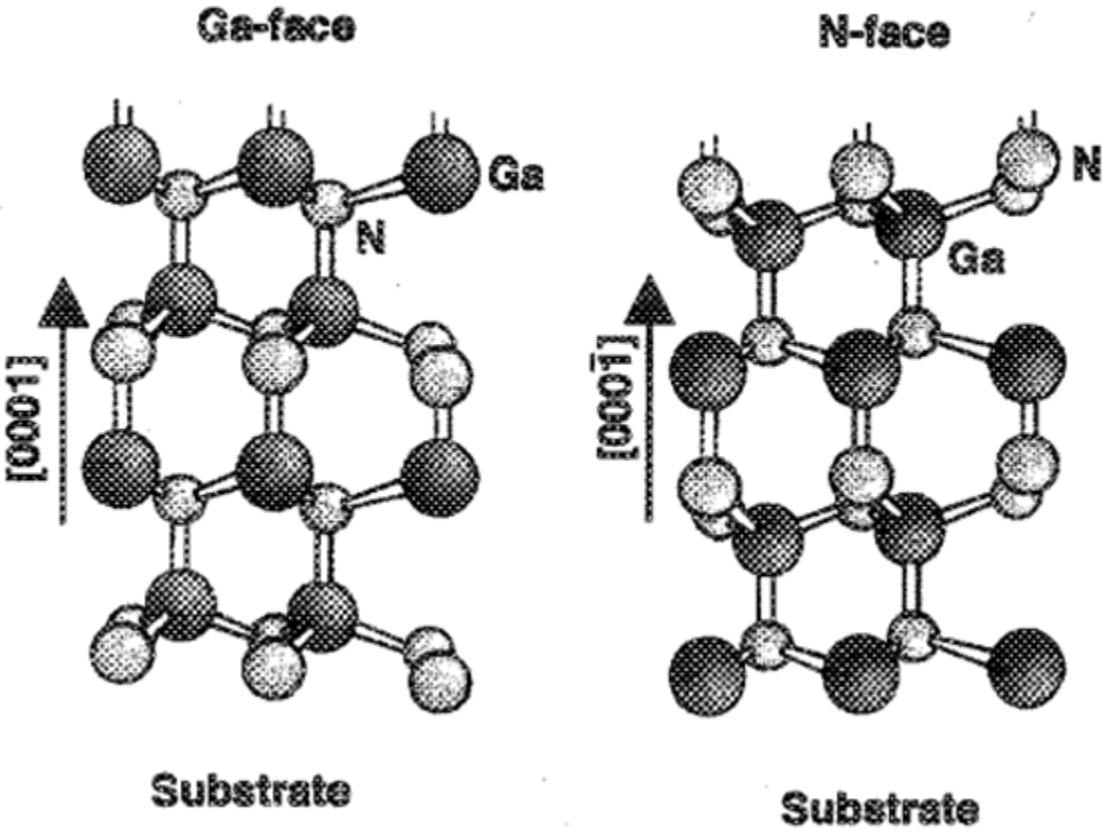

Figure 2.5: Schematic representations of wurtzite GaN, where Ga-face and N-face are indicated by opposite directions [39].

GaN based materials possess excellent transport properties suitable for high power, high temperature and high frequency devices. The electron saturation velocity of GaN is 2.5×10^7 $cm.s^{-1}$ at a field 10^5 Vcm^{-1} [40]. The electron mobility of epitaxial GaN has been recorded at 1000 $cm^2V^{-1}s^{-1}$ for epitaxial layers [41,42]. The value of low temperature mobility in doped GaN is recorded above 7000 $cm^2V^{-1}s^{-1}$ [43]. GaN based materials have high breakdown fields of up to 5×10^6 $V^{-1}cm^{-1}$ [44]. SiC is one wide bandgap semiconductor that possesses a higher thermal conductivity than GaN, which makes it superior to GaN for high temperature devices. However, GaN, with a thermal conductivity greater than 2.1 $Wcm^{-1}°C^{-1}$, enjoys the direct bandgap advantage [45].

The wurtzite (hexagonal) structure GaN based materials are grown along the [0001] direction while the zincblende (cubic) crystals are grown along the [1111] direction, as shown in figure 2.5. These are polar axes, which cause GaN-based semiconductors to contain strong lattice polarization effects. Large spontaneous polarization is suitable for applications in high temperature piezoelectronics and in pyroelectronic sensors. Properties such as piezoelectricity and pyroelectricity are important elements in detector technology. Piezoelectric semiconductors are able to generate electric potentials in response to applied mechanical stress, while pyroelectric materials are capable of generating electric charges in response to heat flow. When heat is applied it changes the temperature of the material by means of thermal convection, diffusion or radiation. GaN and AlN are believed to contain some spontaneous polarization, leading to high piezoelectric constants, which furthermore leads to high piezoelectric polarization in strained films [46].

The pyroelectric response in GaN-based materials results from the piezoelectric effects of temperature-induced strain. There exists a primary piezoelectric effect, which is dominant during fast heat transfer such as the immersion of a device in a medium with high flow velocity. In such a medium, a GaN-based sensor generates a response voltage that is proportional to heat flow. For example, there is a difference in the thermal expansion coefficients of the substrate and the pyroelectric material produces strain in response to temperature changes owing to the applied strain (piezoelectric strain), which in turn generates an electric charge [47]. It has been shown that the pyroelectric voltage coefficient in GaN can be as high as 7×10^5 V/m-K [48] and is

higher than that of the best-known high temperature pyroelectric material, $LiTaO_3$, whose pyroelectric voltage is 5×10^5 V/m-K [49]. In GaN based materials, strong polarization effects result from piezoelectric polarization, which depends on the lattice strain and spontaneous polarization. Spontaneous polarization exerts a strong influence on the electrical properties of heterostructures such as the electron density. Spontaneous polarization arises as a result of large ionicity associated with covalent metal nitrogen bonds and low symmetry in wurtzite material. It also causes an unstable electric field that may decrease or increase the interfacial carrier concentration. In heterostructures where strain is present, the polarization charge is inextricably connected to the present free carriers in the semiconductor. The magnitude of this charge is measured by converting it to the number of electrons: it can be in the mid 10^{13} cm^{-2} level for AlN/GaN interfaces [46]. This is very high compared to AlAs/GaAs heterostructures, where the number of electrons is less than 10% of that of the AlN/GaN structure. AlGaN/GaN devices, in particular, high-electron-mobility-transistor (HEMT), have an extremely large charge density as a result of the two dimensional electron gas (2DEG) formed at the AlGaN/GaN interface, occurring even without doping in the AlGaN. Figure 2.6 shows the energy band of a basic HEMT, indicating the position of 2DEG. Table 2.1 furnishes a summary of some of the properties of III-nitride semiconductors.

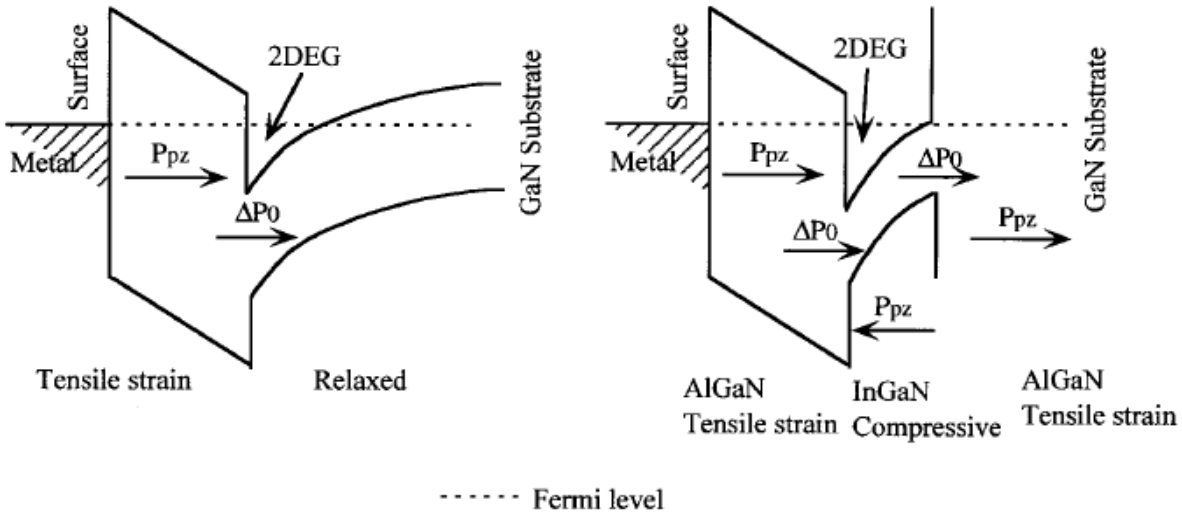

Figure 2.6: AlGaN/GaN structure showing the 2DEG caused by spontaneous and piezoelectric polarization [50].

Table 2.1: Properties of Wurtzite III-Nitrides Semiconductors.

Property	**Units**	**AlN**	**GaN**	**InN**
Crystal Type		Wurtzite	Wurtzite	Wurtzite
Energy Band Gap	eV	6.2	3.39	1.89
Electron Mobility	cm^2/Vs	135	1000 (bulk)	1100
Hole Mobility	cm^2/Vs	15	30	10
Breakdown Fields	V/cm	1.4×10^5	$>5 \times 10^6$	1.4×10^5
Saturation Velocity	cm/s	1.4×10^7	2.5×10^7	2.5×10^5
Thermal Conductivity	W/cmK	2	1.5	6.4×10^{-5}
Lattice Constant, *a*	Å	3.11	3.19	3.54
Lattice Constant, c	Å	4.98	5.18	5.76

2.4 Applications of GaN-based materials.

III-nitrides are suitable semiconductor materials for use in optoelectronic devices, as both emitters and detectors. They can also be used to fabricate high power and high temperature electronic devices [51]. The allowed energy bandgaps of these materials are suitable for band-to-band light generation with colours ranging from potentially red to UV wavelengths, rendering them an advantageous addition to the already existing semiconductor systems for colour displays. It has been demonstrated that nitrides can be used as Bragg reflectors [52], UV detectors [53], UV and visible light emitting diodes (LEDs) for applications in flat panel displays, lighting and indicator lights on devices, advertisements and traffic signals [54]. As coherent sources, lasers are important for high-density optical read-write technologies [55]. The diffraction-limited optical storage density increases approximately quadratically as the probe

laser wavelength is reduced, making the GaN-based materials suitable for coherent sources at lower wavelengths of the electromagnetic radiation. Optical storage enables the storage and retrieval of data in vast quantities. Medical applications of UV LEDs and lasers include surgery [56], phototherapy of neonatal jaundice [57], photodynamic therapy [30], photo-polymerization of dental composites [30], phototherapy of seasonal affective disorder [30], and sterilization [58]. When used in surgery, UV lasers are seen as most suitable due to the fact that UV can sterilize. In photosynthesis, the high brightness LEDs are suitable for the growing of plants and for photo bioreactors [59]. Finally, the LEDs and laser diodes (LDs) are suitable for use in optical measurements such as time domain and frequency domain spectroscopy [60]. Furthermore, exposure to UV-B radiation causes skin cancer to fair skinned people. The use of AlGaN ultraviolet detectors will help prevent such disease, where a handheld device will be able to communicate to user how much ultraviolet radiation was absorbed.

There is great concern all over the world about the contribution of uncontrolled effluents to global warming which is an unexpected change in climate. The effluents stem from aerosols, car fumes, industries and wild fires, and add to the concentration of CO_2 in the atmosphere. When installed in jet engines, cars and furnaces, the UV detectors would monitor and control contaminants for a cleaner environment. In addition, UV detectors operating in the solar-blind region of the electromagnetic spectrum, when made from GaN-based materials, record a high detectivity and are useful in the detection of UV-C (280 nm to 10 nm) and UV-B (320 nm to 280 nm) [61]. UV-C and UV-B are not detectable naturally because the ozone layer is a natural UV filter for all radiation less than 280 nm [35]. It has been observed that power lines emit UV-C radiation as a result of ionization of nitrogen around them.

2.5 Al_xGaN_{1-x} photodetectors

Since the first GaN UV photoconductive photodiode reported by Khan in 1992 [62], all types of photodiode structures have been developed. These are linked directly with the advancement of GaN and AlGaN growth, progress in p-type doping and the improvement of both ohmic and Schottky contact technology. The first developments were focused on the fabrication of visible-blind and solar-blind UV detectors in which the Al mole fraction plays a crucial role in determining the detection band edge [63]. The next stages of development of the photodiodes were focused on the advancement of detector parameters: high responsivity [64], high quantum efficiency [65], high detectivity [66], and UV imaging using focal plane arrays [67]. Photoconductive photodiodes [68], p-n junctions [24], metal-semiconductor-metal (MSM) [69] and Schottky barrier (SB) diodes [55] have already been reported. The success of Schottky barrier photodetectors depends on the structure of both the metallization and the AlGaN used for fabrication. Khan et al. reported the first high quality UV Schottky photodetectors. They used the Cr/Au metal system for the preparation of the ohmic contacts and Ti/Au for Schottky barriers. The spectral responsivity of these detectors reached a maximum value at 365 nm. Miyake et. al. used a Ti/Al structure for the fabrication of ohmic contacts and Ni/Au for Schottky contacts. The transmittance of the Ni/Au electrode in the near UV and VUV region was up to 60 %. The responsivity of the AlGaN detector operating in the UV-VUV wavelength range was found to be 100-265 nm [53].

In recent advances, Tut et. al. demonstrated solar-blind photodetectors with low noise, high detectivity and high quantum efficiency [70]. The AlGaN epitaxial layers were grown on sapphire substrate using MOCVD. A thin nucleation layer of AlN was first deposited on sapphire, to control the cracking of AlGaN. Unintentionally doped GaN mesa isolation with 0.5 μm thickness was grown onto AlN. This was followed by the deposition of a highly doped ($2 \times 10^{18} cm^{-3}$; 0.6 μm) GaN ohmic contact layer. The diffusion barrier, expected to increase the solar blindness of the photodetector, was deposited as a layer of 0.2 μm n-AlGaN. The growth of the Schottky heterostructure was completed with the deposition of a 0.8 μm undoped AlGaN active layer. Ti/Al (100 Å/ 1000 Å) ohmic contacts were deposited onto the highly doped GaN since it was difficult to produce high quality ohmic contacts onto AlGaN. Au Schottky contacts of 100 Å

were deposited onto the active layer. The photodiodes exhibited a low leakage current: less than 3 fA and 10 fA for reverse bias voltages of 12 V and 17 V respectively. The spectral response of solar blind photodetectors was measured at the 250 - 400 nm spectral range. When the applied voltage increased from 5 V to 20 V, the peak responsivity increased from 61 mA/W at 250 nm to 147 mA/W at 256 nm. The responsivity reached saturation for voltages greater than 20 V, indicating a total depletion of the undoped AlGaN absorption layer. A cut-off wavelength of the diodes was reached at 267 nm, which ensures the true solar blindness operation of the diodes. The zero-bias (photovoltaic) quantum efficiency was very low. A maximum quantum efficiency of 71% was measured at 256 nm under 20 V reverse bias.

2.6 Ohmic contacts on AlGaN/GaN

Early studies of ohmic contacts on GaN used Al and Au metallization, which yielded specific contact resistivities in the range of 10^{-4} and 10^{-3} Ωcm [71]. Addition of Ti/Au to Ti/Al improved the specific contact resistivity to 10^{-6} Ωcm [72]. In taking the Ti/Al metal structure further, Wu et al. confirmed that Ti/Al functions very effectively, except at a high annealing temperature [73]. It was realized that at such temperatures, Al melts and tends to form balls on the surface of GaN, increasing the surface's roughness. Rough surfaces are detrimental to the performance of a device because they cause an increase in contact resistivity. As a follow-up on the Ti/Al structure, Fan et al. designed a multilayer ohmic contact, using Ti/Al/Ni/Au (150 Å/2200 Å /400 Å /500 Å) [74]. The measured ohmic contact resistivities were 1.19×10^{-7} and 8.9×10^{-8} Ωcm, respectively. Ti was introduced due to its capability to form a reactive interface with GaN; annealing the metal enhances the formation of TiN as a result of the reaction with GaN. Lack of N from GaN increases the electron concentration through the formation of the N vacancy. Al passivates the GaN surface, while forming a Ti/Al metal layer. It has also been observed that the ratio of Al to Ti in nitrides has an influence on the specific contact resistance. Ti is capable of forming TiN during annealing, which makes the surface highly reactive. During annealing, metallic Ga from GaN has a tendency to diffuse through the metal contact. Al is then used to prevent out-diffusion of Ga to the surface. Thus the Ti/Al system is enough to produce good ohmic contacts as a result of their capability to form thin AlN, TiN and AlTiN at the interface. In addition, it was found that the Ti/Al structure reduces the

contact resistance by varying conditions such as the annealing and ambient temperature. A Ti/Al/Ni/Au structure has been successfully used in optimizing the specific contact resistance.

Similar metal combinations have been used to make ohmic contacts on AlGaN, with Ti/Al structures being kept as basic [75]. Ti/Al/Ti/Au (200 Å, 1000 Å, 450 Å, 600 Å) combinations were reported, with a Ti layer deposited onto AlGaN, thus enhancing adhesion to the semiconductor. It was also found the reaction of Ti with residual surface oxide to form TiO_2 is beneficial to the device being fabricated. TiO_2 has a bandgap of 3.05 eV, which is smaller than the GaN bandgap (3.5 eV). The TiO_2 bandgap compared to other surface oxides on AlGaN, Ga_2O_3 (bandgap 4.4 eV), and Al_2O_3 (bandgap of 8.8 eV) reduces surface states. Using Ti alone for ohmic contact formation would require annealing temperatures as high as 900°C via TiN formation. The interaction of Al with N in AlGaN occurs at lower temperatures than the TiN formation; hence an ohmic contact is formed by Ti/Al/Ti combinations, when Al diffuses through the surface Ti layer. Au is used to protect oxidation of surface metal, whether it is Ti or diffused Al. Hence, Ti/Al/Ti/Au combinations are used with modifications to the second Ti layer replaced by Mo, Ni, and Pt [76]. All these combinations are regarded as reducing contact resistivity.

REFERENCES

[1] Compound Semiconductor, March 2005, p12.

[2] Maruska H. P. and Tietjen J. J., The preparation and properties of vapor-deposited single-crystalline GaN, Applied Physics Letters **15** (1969) 329.

[3] Liu L. and Edgar J. H., Substrates for gallium nitride epitaxy, Material Science and Engineering **R37** (2002) 61.

[4] Lester S. D.,Ponce F. A., Craford M. M. G., Steigerwald D. A., High dislocation densities in high efficiency GaN-based light-emitting diodes, Applied Physics Letters **66** (1995) 1249.

[5] Ponce F. A., Cherns D., Young W. T.and Steeds J. W., Characterization of dislocations in GaN by transmission electron diffraction and microscopy techniques, Applied Physics Letters **69** (1996) 770.

[6] Mohammad S. N., Salvador A. A. and Morkoc H., Emerging gallium nitride based devices, Proceeding IEEE **83** (1995) 1306.

[7] Morkoc H., Comprehensive characterization of hydride VPE grown GaN layers and templates, Material Science Engineering **R33** (2001) 135.

[8] Uchida K., Watanabe A., Yano F., Kouguchi M., Tanaka T. and Minagawa S., Nitridation of sapphire substrate surface and its effects on the growth of GaN, Applied Physics Letters **79** (1996) 3487.

[9] Waltereit P. and Brandt O., Influence of AlN nucleation layers on growth mode and strain relief of GaN grown on 6H-SiC(0001) Applied Physics Letters **74** (1999) 3660.

[10] Rubin M and Weber E, US Patent # IB 1290

[11] http://projects.ece.utexas.edu/ece/mrc/groups/street_mbe/mbechapter.html

[12] Wang J., Guo L. W., Jia H. Q., Xing Z. G., Wang Y., Chen H. and Zhou J. M., Lateral epitaxial overgrowth of GaN films on patterned sapphire substrates fabricated by wet chemical etching, Thin Solid Films **515** (2006) 1727.

[13] Gibart P., Metal Organic Vapour Phase Epitaxy of GaN and Lateral Overgrowth, Progress Reports Physics **67** (2004) 667.

[14] Lee I-H, Polyakov A. Y, Smirnov N. B., Govorkov A. V, Markov A. V., Pearton S. J., Deep-level studies in GaN layers grown by epitaxial lateral overgrowth, Thin Solid Films **516** (2008) 2035.

[15] Park S-E., Han W. S., Lee H. G. and Byungsung O., Effects of native defects on electrical and optical properties of undoped polycrystalline GaN, Journal of Crystal Growth **253** (2003) 107.

[16] Van de Walle C. G., Stampfl C. and Neugebauer J., Deep level related yellow luminiscence in p-GaN grown by MBE, Journal of Crystal Growth **189/190** (1998) 505.

[17] Zhang J-P., Sun D-Z., Wang X-L., Kong M-Y. Zeng Y-P., Li J-M. and Lin L-Y., Hydrogen contaminants and its correlation with background electrons in GaN, Semicondunctor Science Technology **14** (1999) 403.

[18] Ogino T and Aoki M,Mechanisms of yellow luminescence in GaN, Japanese Journal Physics. (Japan), **19** (1980) 2395.

[19] Saarinen K, Observations of native Ga vacancies by positron annihilation, Physical Review Letters **79 (**1997) 3030.

[20] Reynolds D. C., Look D. C., Jogai B., Van Nostrand J. E., Jones R. and Jenny J., Sources of yellow luminescence in GaN grown by gas–source molecular beam epitaxy and the green luminescence band in sigle crystals ZnO, Solid State Communication. 1**06** (1998) 701.

[21] Nyk M., Jablonski J. M., Strek W. and Misiewicz J., Yellow emission of GaN nanocrystals embedded in silica xerogel matrix, Optical Material **26** (2004) 133.

[22] Hacke P., Detchprohm T.,Hiramatsu K., Sawaki N., Tadatomo K. and Miyake K., Degradation mechanisms in AlGaN/InGaN/GaN light sources, Applied Physics Letters **76** (1994) 304.

[23] Hacke P., Nakayama H., Detchprohm T.,Hiramatsu K. and Sawaki N. Deep levels in upper band-gap region of lightly Mg-doped GaN, Applied Physics Letters **68** (1996) 1362.

[24] Auret F. D., Goodman S. A., Koschnick F. K., Spaeth J.-M, Beaumont B. and Gibart P, Proton bombardment induced electron traps in epitaxialy grown n-GaN, Applied Physics Letters **74**, (1999) 407

[25] Eiting C. J., Grudowski P. A. and Dupuis R. D.P- and N-type doping of GaN and AlGaN epitaxial layers grown by metalorganic chemical vapour deposition, Journal of Electronic Material. **27** (1998) 206.

[26] Calleja E., **Sanchez**-Garcia M. A., Calle F., Naranjo F. B., Munoz E., Jahn U., Ploog K., Calleja J. M., Sarinen K. and Hautojarvi P., Molecular beam epitaxy growth and doping of III-nitrides on Si(111): layer morphology and doping efficiency, Material Science and Enginering **B82** (2001) 2.

[27] Binet F., Duboz J.Y., Rosencher E., Scholz F., and Hãrle V., Mechanisms of recombinations in GaN photodetectors, Applied Physics Letters **69** (1996) 1202.

[28] Huang Z.C., Mott D.B., Shu P.K., Zhang R., Chen J.C., and Wickenden D.K., Optical quenching of photoconductivity in GaN photoconductors, Applied Physics Letters **82** (1997) 2707.

[29] Monroy E., Garrido J.A, Muñoz E., Izpura I., Sánchez F.J., Sánchez-García M.A., Calleja E., Beaumont B., and Gibart P., High performance GaN p-n junctions photodetectors for solar ultraviolet applications, Semiconductor Science and Technology **13** (1998) 1042.

[30] Huang Z.C., Mott D.B., Shu P.K., Chen J.C., and Wickenden D.K., Improvement of metal-semiconductor-metal GaN photodetectors, Journal of Electronic Material **26** (1997) 330.

[31] Kozodoy P., Ibbetson J.P., Marchand H., Fini P.T., Keller S., Speck J.S., DenBaars S.P, and. Mishra U.K, Electrical characterization of GaN p-n junctions with and without p-n junctions, Applied Physics Letters **73,** (1998) 975.

[32] Parish G., Keller S., Kozodoy P., Ibbetson J. P., Marchand, H., Fini P. T, Fleischer S.B., DenBaars S. P., Mishra U. K. and Tarsa E.J., High performance (Al,Ga)N-based solar-blind ultraviolet p-i-n detectors on laterally overgrown GaN, Applied Physics Letters **75** (1999) 247.

[33] Vurgaftman I., Meyer J. R. and Ram-Mohan L. R. J., Band parameters for III-V semicobnductors and their alloys, Applied Physics Letters **89** (2001) 5815.

[34] Davvydov V. Y., Klochikin A. A., Emstev V. V., Kurdyukov D. A., Ivanov S. V., Vekshin V. A., Bechstedt F., Furthmuller J., Aderhold J., Graul J., Mufrui A. V., Harima H.,

Hashimoto A., Yamomoto A., Haller E. E., Bandgap of hexagonal InN and InGaN alloys, Physica Status Solidi (b) **234** (2002) 787.

[35] Levinshtein M. E., Rumyantsev S. L., and Shur M. S., Editors "Properties of advanced Semiconductor Materials: GaN, AlN, InN, BN, SiC, and SiGe",John Wiley and Sons, New York (2001).

[36] Davvydov V. Y., Klochikin A. A., Seisyan R. P., Emstev V. V., Ivanov S. V., Bechstedt F., Furthmuller J., Harima H., Mudryi A. V., Aderhold J., Semchinova O., and Graul J., Absorption and emission of hexagonal InN: Ebidence of narrow fundamental bandgap, Physica Status Solidi (b) **229** (2002) R1.

[37] Tut T., Butun B., Gokkavas M., Ozbay E, Solar-blind AlxGa1-xN-based avalanche photodiodes, Applied Physics Letters **87** (2005) 223502.

[38] Monroy E., Calle F., Munoz E., Omnes F. Gibart P. and Munoz J. A., Applied Physics Letters **73** (1999) 1171

[39] Ambercher O., Smart J., Shealy J. R., Wemann N. G., Chu K., Murphy M., Schaff W. J., Eastman L. F., Dimitrov R., Wittmer L., Stutzmann M., Rieger W. and Hilsenbeck J., Journal Applied Physics **85** (1999) 3222.

[40] Albrecht J. D., Wang R. P., Ruden P. P., Farahmand M. and Brennan K. F., Electron transport characteristics of GaN for high temperature device modeling, Journal of Applied Physics **83** (1998) 4777.

[41] Heying B., Smorchkova I., Poblenz C., Elsass C., Fini, B. Denbaars S., Mishra U. and Speck J. S., Optimization of surface morphologies and electron mobilities in GaN by plasma-assisted molecular beam epitaxy, Applied Physics Letters **77** (2000) 2885.

[42] Ambacher O., Smart J., Shealy J. R., Wenmann N. G., Chu K., Murphy M., Schaff W. J., Eastman L. F., Dimitrov, R., Wittmer L., Stutzman M., Rieger W. and Hilsenbeck J., Two-dimensional electron gases induced by spontaneous and piezoelectric polarization charges in N- and Ga-phase AlGaN/GaN, Journal of Applied Physics **85** (1999) 3222.

[43] Morkoc H., Cingolani R., Lampbrecht W., Gil B., Jiang H-X, Lin J., Pavlidis D. and Shenai K., Material properties of GaN in the context of electronic devices, MRS Internet Journal Nitride Semiconductors **R 4S1** (1999) G1.2.

[44] Harima H., Properties of GaN and related compounds studied by means of Raman scattering, Journal of Physics: Condense Matter **14** (2002) R967.

[45] Florescu D. I., Asnin V. M. and Pollak F. H., Thermal conductivity measurements of GaN and AlN, Compound Semiconductor **7** (2001) 62.

[46] Bernardini F., Fiorentini V., and Vanderbilt D., Photoluminiscence in n-doped In0.1Ga0.9N/In0.01Ga.099N multiple quantum wells, Physical Review B **56** (1997) R10024.

[47] Shur M. S., Bykhovski A. D. and Gaska R., Pyroelectric and Piezoelectric properties of GaN-based materials, MRS Internet Journal Nitride Semiconductors Res. **4S1** (2000) G1.6.

[48] Shur M. S. and Khan M. A., AlGaN/GaN doped channel heterostructure field effect transistors, Physica Scripta **T69** (1997) 103.

[49] Fraden J., Handbook of Modern Sensors, Springer, New York (1996) 536.

[50] Morkoς H., Cingolani R. and Gil B., " Polarization effects in nitride semiconductor device structures and performance of modulation doped field effect transistors, Solid State Electronic, **43** (1999) 1753

[51] Yoshida S., Ishii H., Li J.., Wang D., and Ichikawa M., A high-power AlGaN/GaN heterojunctions field effect transistor, Solid State Electronics **47** (2003) 589.

[52] Fritz I. J. and Drummond T. J., AlGaN quarter-wave reflector stack grown by gas-source MBE on (100)GaAs, Electronic Letters **31** (1995) 68.

[53] Munoz E., Monroy E., Pau J. L., Calle F., Omnes F. and Gibart P., III-V nitrides and UV detection, Journal of Physics: Condense Matter **13** (2001) 7115.

[54] Tsao J. Y., Solid-State lighting : lamps, chips and materials fo tomorrow, IEEE Circuits & Devices **20** (3) (2004) 28.

[55] Miyajima T., Tojyo T., Takeharu A., Katsunori Y., Kijima S., Hino T., Takeya M., Uchida S., Tomiya S., Funato K., Asatsuma T., Kobayashi T and Ikeda M., GaN blue laser diode, Journal of Physics: Condense Matter **13** (2001) 7099.

[56] Mead R.D.,Miyake C. I. and Lowenthal D. D., US Patent **5**,742, 626 (1998).

[57] Vreman H. J., Wong R. J. and Stevenson D. K., Phototherapy: Current methods and future directions, Seminars in Perinatology, **28** (2004) 326.

[58] Shodeen K., Davenpot S. and Melgaard H. L., Patent 5,446,289, (1995).

[59] Day T. A., Ruhland C. T. and Xiong F. S., Multiple trophic levels in UV-B assessments-completing the ecosystem, Journal of Photochemistry and Photobiology B **62** (2001) 78.

[60] Ishida M., Ogawa M., Orita K., Imafuji O., Yuri M., Sugino T. and Itoh K., Drastic reduction of threading dislocations in GaN grown on groove stripe structure, Journal of Crystal Growth **221** (2000) 345.

[61] Liu S-S., Li P-W., Lan W. H. and Lin W-J., Improvements of AlGaN/GaN p-i-n UV sensors with graded AlGaN layer for the UV-B (280-320 nm) detection, Material Science and Engineering. B **122** (2005) 196.

[62] Asif-Khan M., Kuznia J. N.,Olson D. T., van Hove J. M. and Blasingame M., High responsivity photoconductive ultraviolet sensors based on insulating single-crystal GaN epilayers, Applied Physics Letters **60** (1992) 2917.

[63] Shur M. S. and Zukauskas A., (Eds) UV Solid State Emitters and Detectors Kluwer, Dordrecht, (2004).

[64] Miyake H., Yasukawa H., Kida Y., Ohta K., Shibata Y., Motogaito A., Hiramatsu K., Ohuchi Y., Tadatomo K., Hamamura Y. and Fukui K., High performance Schottky UV detectors (265-100 nm) using n-Al0.5Ga0.5N on AlN epilayers, Physica Status Solidi (a) **200** (2003) 151.

[65] Wong M. M., Chowdhury U., Collins C. J., Yang B., Denyszyn J. C., Kim K. S., Campbell J. C., and Dupuis R. D., High quantum efficiency AlGaN /GaN solar-blind photodetectors grown by metaorganic chemical vapour deposition, Physica Status Solidi (a) **188** (2001) 333.

[66] Wang C. K., Chang S. J., Su Y. K., Chiou Y. Z., Lin T. K., Liu H. L., and Tang J. J., High detectivity GaN metal-semiconductor-metal UV photodetectors with transparent tungsten electrodes, Semiconductor Science and Technology **20** (2005) 485.

[67] Huang T. Z.,Mott D. B., and Lah A. T., Development of 256x256 GaN ultraviolet imaging arrays, Proceedings SPIE **3764** (1999) 254.

[68] Shen B., Yang K., Zang L., Chen Z-Z., Zhou Y-G., Chen P., Zhang R., Huang Z-C., Zhou H-S and Zheng Y-D., Study of photocurrent properties of GaN ultraviolet photoconductor grown on 6H-SiC Substrate, Japanese. Journal of Applied Physics **38** (1999) 767.

[69] Chung S-J., Hung H., Lin C-Y.,Wu M-H.,Kuan H.and Lin M-R., AlGaN Ultraviolet Metal-Semiconductor-Metal Photodetectors with Low-Temperature-Grown Cap Layers, Japanese. Journal of Applied Physics **46** (2007) 2471.

[70] Tut T, Biyikli N., Kimukin I., Kartaloglu T., Aytur O., Unlu M. S. and Ozbay E., High band-width-efficiency solar-blind AlGaN Schottky photodiodes with low dark current, Solid State Electronics **49** (2005) 117.

[71] Foresi J. S. and Moustakas T. D., Metal contacts to GaN, Applied Physics Letters **62,** (1993) 2859.

[72] Lin M. E., F. Y. Huang, Fan Z, Allen L., and Morkoc H., Low resistance ohmic contacts on wide band-gap GaN, Applied Physics Letters **64** (1994) 1003.

[73] Wu Y., Jiang W., Keller B., Keller S., Kapolneck D., Denbaars S. and Mishra U., Low luminescence ohmic contact to n-GaN with a separate layer method, Solid State Electonics **41** (1997) 75.

[74] Fan Z., Mohammad S. N., Kim W., Aktas O., Botchkarev A. E. and Morkoc H., Very low resistance multilayer Ohmic contact to n-GaN, Applied Physics Letters **68** (1996) 1672.

[75] Davvydov A. V., Motayed A., Boettinger W. J., Gates R. S., Xue Q. Z., Lee H. C. and Yoo Y. K., Combinatorial optimization of Ti/Al/Ti/Au ohmic contacts to n-GaN, Physica Status Solidi (c) **2** (2005) 2551.

[76] Selvanathan D. Zhou L., Kumar V and Adesida I., Low resistance Ti/Al/Mo/Au ohmic contacts for AlGaN/GaN heterostructure field effect transistors, Physica Status Solidi (a) **194** (2002) 583.